Three-particle cluster structure above $E_x = 11$ MeV in ^{15}N

C. Lee,[1,*] J. A. Liendo,[2] P. D. Cathers,[1] N. R. Fletcher,[1] K. W. Kemper,[1] and P. L. Kerr[1,†]
[1]*Department of Physics, Florida State University, Tallahassee, Florida 32306-4350*
[2]*Universidad Simón Bolívar and I.V.I.C., Caracas, Venezuela*
(Received 26 August 1998; published 23 July 1999)

^{12}C(^{7}Li,α) angular distributions have been obtained for 16 states in ^{15}N at $E(^7\mathrm{Li}) = 52.5$ MeV. Also, ^{12}C($^6\vec{\mathrm{Li}}$,^{3}He) angular distributions and vector analyzing powers have been measured at $E(^6\vec{\mathrm{Li}}) = 50$ MeV. Finite-range distorted-wave Born-approximation (FRDWBA) triton cluster transfer calculations are able to describe the (^{7}Li,α) data for transfer to states with known J^π values. Comparison with known levels in ^{19}F suggests that the ^{12}C(^{7}Li,α) reaction selectively populates negative parity states. FRDWBA calculations support this idea. Several previously suggested J^π levels are confirmed and new J^π values are proposed for six other levels. The previously observed ($^6\vec{\mathrm{Li}}$,^{3}He) J dependence has been used along with coupled-channel Born-approximation calculations to confirm the J^π values for states in ^{15}N. [S0556-2813(99)08008-5]

PACS number(s): 21.60.Gx, 25.70.Hi, 27.20.+n

I. INTRODUCTION

Early [1–3] three-particle transfer reaction studies with ^{12}C and ^{16}O as targets showed tremendous selectivity in the states populated in the final nuclei ^{15}N and ^{19}F. A relatively simple triton cluster model [4,5] was shown to describe some of the strongly populated states in these nuclei. However, the lack of definite spin and parity assignments for levels at higher excitation energies has hampered the further development of simple cluster models for these nuclei, especially for the case of ^{15}N. The present work was undertaken to provide new information on the three-particle cluster structure of ^{15}N.

The ^{12}C(α,p)^{15}N [3,6] and the ^{12}C(^{6}Li,^{3}He)^{15}N [7,8] reactions are highly selective in the states populated, with both reactions populating the same states with roughly the same relative intensities. The ^{12}C(^{7}Li,α) reaction also selectively excites states in ^{15}N, but with considerably different strengths [9,10] when compared to the (α,p) and (^{6}Li,^{3}He) reactions. Also, the ^{12}C(^{7}Li,α) reaction excites states in ^{15}N that are either weakly populated or perhaps not populated at all by the (α,p) and (^{6}Li,^{3}He) reactions. While the (α,p) and (^{6}Li,^{3}He) reactions should favor the population of high spin states, because they are quite angular momentum mismatched, the (^{7}Li,α) reaction is just the opposite and should favor low spin states. Such a simple interpretation of the (^{7}Li,α) reaction does not seem to be possible, since both high and low spin states appear in the spectrum [11].

The present work reports cross sections and angular distributions for the ^{12}C(^{7}Li,α) reaction for a ^{7}Li bombarding energy of 52.5 MeV. Cross section and vector analyzing powers have also been measured for the ^{12}C($^6\vec{\mathrm{Li}}$,^{3}He) reaction for $E(^6\vec{\mathrm{Li}}) = 50$ MeV, to aid in the assignment of spins and parities for the observed three-particle cluster states. This higher ^{6}Li energy was chosen because an earlier study of ^{12}C($^6\vec{\mathrm{Li}}$,^{3}He) at $E(^6\vec{\mathrm{Li}}) = 34$ MeV had shown [8] that the measured vector analyzing powers are sensitive to the J^π of the transferred cluster, but the bombarding energy was not high enough to strongly excite states above about 13 MeV in excitation in ^{15}N. The same difference in selectivity between the (^{6}Li,^{3}He), (α,p) and (^{7}Li,α) reactions on an ^{16}O target for populating states in ^{19}F has been reported [1,12–15]. The studies of ^{19}F have resulted in considerably better spin, parity, and cluster configuration assignments than those for ^{15}N. The current knowledge of the selectively populated states in ^{19}F has been combined with both finite-range distorted-wave Born-approximation (FRDWBA) and coupled-channel Born-approximation (CCBA) calculations in the present work to assign spin-parity and possible cluster structures for the selectively excited states in ^{15}N. Calculations and data are presented for excited states up to 20 MeV in excitation in ^{15}N.

II. EXPERIMENT

A. ^{12}C(^{7}Li,α)^{15}N

The ^{12}C(^{7}Li,α)^{15}N reaction was studied using a 52.5 MeV ^{7}Li^{3+} beam from the Florida State University Tandem/LINAC Accelerator. The ^{12}C target was 100 μg/cm^2 thick and self-supporting. The average beam intensity throughout the study was about 25 e nA. The identification of the α particles was achieved using a pair of ΔE-E detector telescopes. Narrow collimators which gave angle openings $\pm 0.16°$ and $\pm 0.37°$ were put in front of the detectors to minimize kinematic broadening of the peaks in the spectra. The two telescopes, each separated by 7.5 laboratory degrees, were mounted on a moving arm. Spectra were taken at the laboratory angles of 8°, 11°, 14°, 15.5°, 18.5°, 21.5°, 23°, 27°, and 30.5° with these two telescopes. The linac rebuncher was used to improve the beam-energy resolution so that the total-energy resolution obtained in the sample spectrum shown in Fig. 1 was about 125 keV. The elastic scattering of the ^{7}Li beam was measured at the same time with a monitor detector positioned at 15°, and both elastic

*Present address: Department of Physics, Seoul National University, Seoul 151-742, Korea.
†Present address: Los Alamos National Laboratory, MSJ561, Los Alamos, NM 87545.

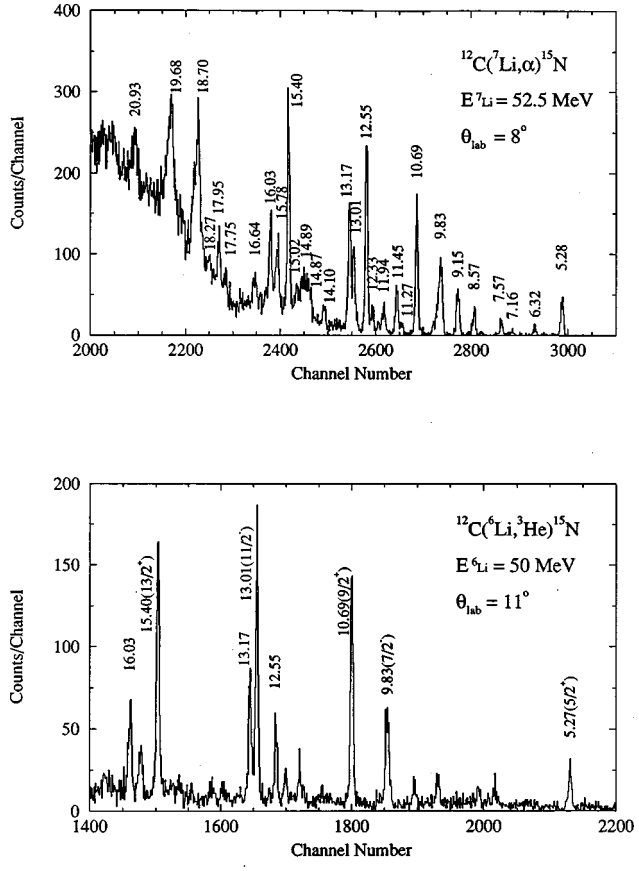

FIG. 1. Sample spectra for the ^{12}C(^{7}Li,α) and ^{12}C(^{6}Li,^{3}He) reactions.

scattering and α particles were measured simultaneously with the telescopes at the laboratory angles of 20°, 21°, and 22°. From these data, the (^{7}Li,α) absolute cross section was obtained by normalizing the measured relative elastic scattering angular distribution to optical model calculations that used parameters that were obtained from 48 MeV elastic scattering [16]. The parameters are listed in Table I. The error in the absolute cross section for the ^{12}C(^{7}Li,α) reaction is estimated to be $\pm 12\%$ based on the range of values obtained for these cross sections from several different runs.

A typical α-energy spectrum for the ^{12}C(^{7}Li,α) reaction is shown in Fig. 1. Selective population of states is found, similar to previous studies [9,10]. The peak identifications are based on the spectrum in Ref. [10], since the beam energy and detecting angles of the current spectra are comparable to those in that spectrum. Also, the better energy resolution of Ref. [10], 80 keV, allowed the peak energies to be more easily determined for spectral regions with closely spaced peaks. An internal calibration of the present data using accepted ^{15}N excitation energies was consistent with these values. Angular distributions were determined for peaks at excitation energies 5.28, 6.32, 7.57, 8.57, 9.15, 9.83, 10.69, 11.45, 12.55, 13.01, 13.17, 14.10, 15.40, 16.03, 17.95, and 19.68 MeV.

B. ^{12}C($^{6}\vec{\text{Li}}$,^{3}He)^{15}N

The FSU optically pumped polarized Li ion source produced the vector polarized ^{6}Li beam used in this work. The polarized ^{6}Li beam from the source was accelerated by the Tandem/LINAC system to produce a $^{6}\vec{\text{Li}}^{3+}$ beam of 100 e nA on target at $E(^{6}\text{Li}) = 50$ MeV. The typical on-target beam polarization was $t_{10} = 1.02 \pm 0.05$. The calibration data of Kerr *et al.* [17] was used to determine the on-target beam polarization. The nucleus ^{6}Li has a ground state spin of 1 so that the three magnetic substates of the beam can be $M_I = 1,0,-1$. The present data were taken by cycling every 2 min between three states of polarization: polarization off and the two magnetic substates $M_I = 1,-1$.

The details of the detectors, scattering chamber, and targets used in this work are the same as those used in a previous work [17]. Again, the linac rebuncher was used to im-

TABLE I. Potential parameters used in the transfer calculations.

	V_0 (MeV)	r_R (fm)	a_R (fm)	W_0 (MeV)	r_I (fm)	a_I (fm)
^{7}Li+^{12}C [a]	145.6	1.22	0.83	12.09	2.22	0.69
α+^{15}N [b]	179.0	1.40	0.57	3.0	1.50	0.60
α+t [c]	searched	1.80	0.70			
t+^{12}C [d]	searched	1.25	0.65			
^{6}Li+^{12}C [e]	N=0.985			8.5	2.35	0.63
^{3}He+^{15}N [f]	276.1	1.15	0.65	16.7	1.43	0.62
^{3}He+t	searched	1.73	0.45			
t+^{12}C	searched	1.80	0.65			

[a]Taken from Ref. [10].

[b]Parameters were determined by obtaining the best description of the experimental data for the 10.67 MeV ($\frac{9}{2}^{+}$) and 13.01 MeV ($\frac{11}{2}^{-}$) states with FRDWBA calculations.

[c]Taken from Ref. [22].

[d]Taken from Ref. [23].

[e]Double folded real potential from Ref. [30].

[f]Parameters were determined by obtaining the best description of the 10.69 MeV and 13.01 MeV data with CCBA calculations.

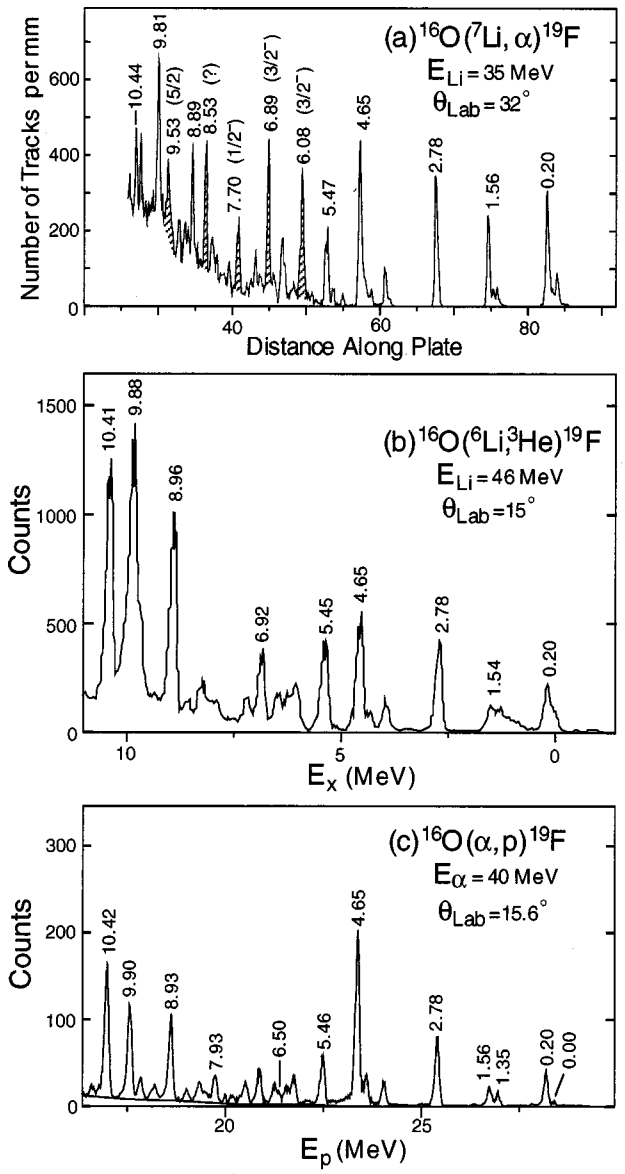

FIG. 2. Spectra for the ^{16}O(^{7}Li,α) [12], ^{16}O(^{6}Li,^{3}He) [14], and ^{16}O(α,p) [15] reactions. These spectra show that ^{19}F states are populated by ^{16}O(^{7}Li,α) with relative intensities which are different from the (^{6}Li,^{3}He) and (α,p) reactions just as observed in Fig. 1.

prove the beam-energy resolution which then resulted in the observed total-energy resolution of 110 keV for the spectrum in Fig. 1. The unpolarized angular distribution data were obtained from the polarization off runs. The absolute cross sections were found by collecting the transfer and ^{12}C+^{6}Li elastic data simultaneously at several angles and then using the same normalization constant between the elastic data and the previously determined elastic cross section [17] for the transfer data. The absolute error in the cross sections is $\pm$12%, and arises primarily from the uncertainty in the elastic cross section, while that for the vector analyzing powers is $\pm$10%, arising from the variation of the observed beam polarization during the runs ($\pm$5%) and the overall on-target beam polarization calibration of ($\pm$8%).

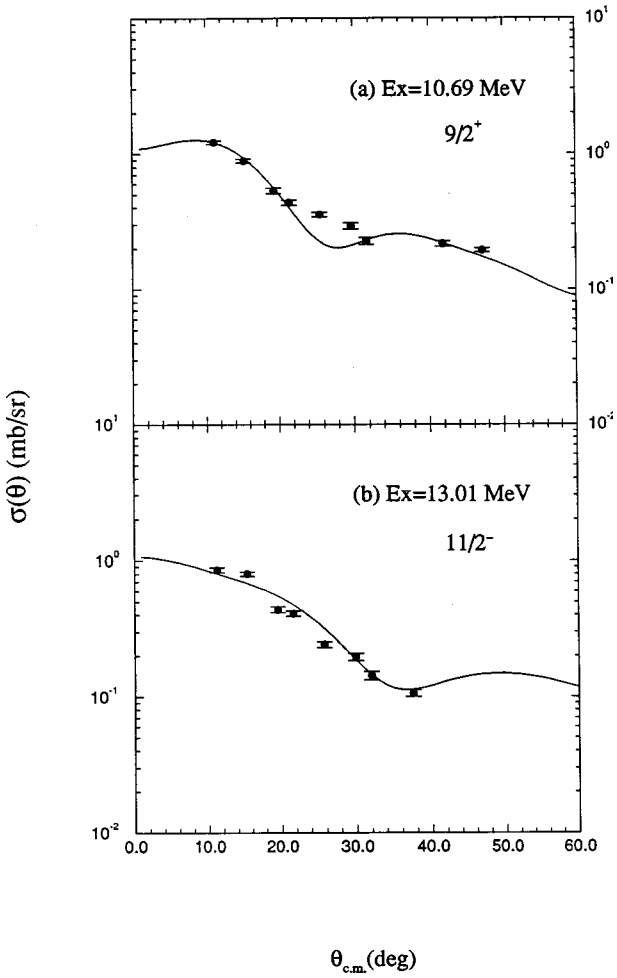

FIG. 3. The solid lines are FRDWBA ^{12}C(^{7}Li,α) test calculations that show that transfers to states with well established J^{π} values can be described.

III. COMPARISON OF DATA SETS

As can be seen in Fig. 1, one major difference between the ^{12}C(^{7}Li,α), and ^{12}C(^{6}Li,^{3}He) reactions is the very different population strengths of the 13.17 and 12.55 MeV peaks relative to the one at 10.69 MeV. In both (^{6}Li,^{3}He) and (α,p), these two states are weaker than the one at 10.69 MeV whereas in ^{12}C(^{7}Li,α) they are stronger. In addition, peaks are selectively and strongly populated up to 21 MeV in excitation in the (^{7}Li,α) reaction, but not in either (^{6}Li,^{3}He) or (α,p). An early work [18] on the cluster structure of ^{15}N suggested that states with similar shell model configurations exist in both ^{15}N and ^{19}F. For comparison, spectra produced by the reactions ^{16}O(^{7}Li,α) [12], ^{16}O(^{6}Li,^{3}He) [14], and ^{16}O(α,p) [15] are shown in Fig. 2. As can be seen, the ^{16}O(^{6}Li,^{3}He) and ^{16}O(α,p) reactions produce spectra that are similar, whereas ^{16}O(^{7}Li,α) excites states with different relative strengths from the latter two reactions. Perhaps the major difference in the three reactions leading to ^{19}F is the strong population of low spin negative parity states by the ^{16}O(^{7}Li,α) reaction. Note in particular the selective strength of the 6.09, 6.89, and 7.70 MeV peaks in the (^{7}Li,α) spectrum when compared with those from (α,p) and (^{6}Li,^{3}He).

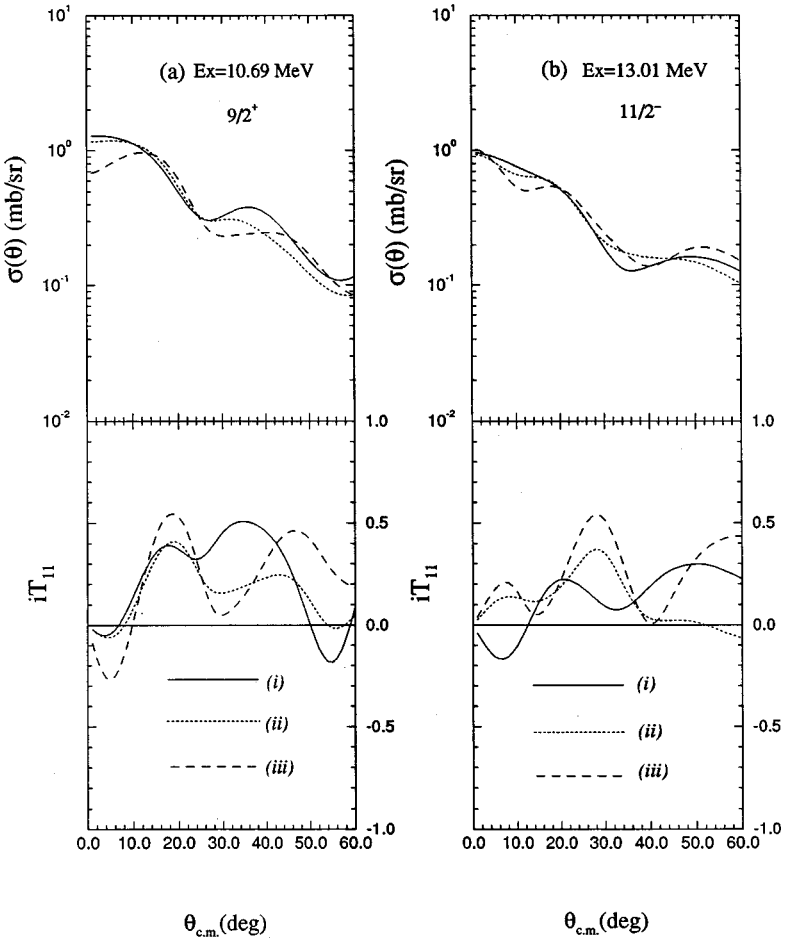

FIG. 4. FRDWBA (i) and CCBA (ii) and (iii) calculations that include (ii) coupling between the ground ($\frac{3}{2}^-$) and first excited state ($\frac{1}{2}^-$) in ^{7}Li but no transfer from the $\frac{1}{2}^-$ state and calculations (iii) that include coupling between the states in ^{7}Li and transfer from the excited $\frac{1}{2}^-$ state in ^{7}Li. While the angular distribution FRDWBA and CCBA calculations are relatively insensitive to whether projectile excitation is included, the iT_{11} calculations can clearly distinguish between the different calculations, especially at forward angles for the 13.01 MeV, $\frac{11}{2}^-$ transition.

The spins and parities of these states are identified in Refs. [12,14] to be $\frac{3}{2}^-$ (6.09 MeV), $\frac{3}{2}^-$ (6.89 MeV), and $\frac{1}{2}^-$ (7.70 MeV) with $(sd)^2(fp)^1$ configurations. It has not been possible to associate the new states observed at 8.53 and 9.53 MeV by $(^7\mathrm{Li},\alpha)$ with known states yet because of the high density of nearby levels. Comparison with the ^{19}F observations would suggest that the 12.55 and 13.17 MeV states in ^{15}N have relatively low spin, negative parity, and a cluster structure of $(sd)^2(fp)^1$.

IV. DWBA AND CCBA CALCULATIONS

A. ^{12}C(^{7}Li,α)^{15}N

Amazingly, there have been very few studies published that determine if $(^7\mathrm{Li},\alpha)$ angular distribution data can be described by finite-range DWBA calculations. The forward angle angular distribution data for the strong positive parity states populated by the $^{16}\mathrm{O}(^7\mathrm{Li},\alpha)$ reaction at a bombarding energy of 20 MeV were shown to be well described by FRDWBA calculations [13,19]. The larger angle data seem to contain both cluster exchange and compound nucleus contributions. No calculations for the $^{12}\mathrm{C}(^7\mathrm{Li},\alpha)$ reaction seem to have been previously published.

To test proposed structures for the states in ^{15}N excited by the $^{12}\mathrm{C}(^7\mathrm{Li},\alpha)$ reaction, FRDWBA angular distribution calculations have been carried out with the computer code DWUCK5 [20]. In these calculations, it is assumed that the $(^7\mathrm{Li},\alpha)$ reaction can be considered to be a direct triton-transfer reaction. Multiple values of the transferred orbital angular momentum are allowed for each final state since the triton occupies a relative p state in the ^{7}Li system. A cluster configuration of $(sd)^3$ $[3p\text{-}4h]$ was assumed for the positive parity ^{15}N states with $2N+L=6$ for the bound state quantum numbers, while $p^1(sd)^2$ $[2p\text{-}3h]$ and $2N+L=5$ was assumed for the negative parity states. Other configurations were also used for certain states and they will be discussed later.

Initial optical model parameters for generating the $\alpha+^{15}$N exit channel distorted waves were taken from a work [21] that measured large angle α scattering by the ^{15}N nucleus. These parameters were then modified for transfer to highly excited states in ^{15}N by obtaining the best fit to the transfer data to the known $\frac{11}{2}^-$ and $\frac{9}{2}^+$ states at 13.01 MeV and 10.70 MeV excitation, respectively. The best fit calculations and data are shown in Fig. 3, with the parameters listed in Table I. Theoretical angular distributions were then generated by FRDWBA calculations for all other observed ^{15}N states with the parameters listed in Table I. The radial parts of the triton bound state wave functions in the ^{7}Li projectile and the ^{15}N nucleus are also calculated from real Woods-Saxon potentials, and are taken from the investigations of Kukulin *et al.* [22] and Kammuri *et al.* [23], respectively. The values of the real depth parameters V_0 were found under the assumption that the triton is a single particle bound to a

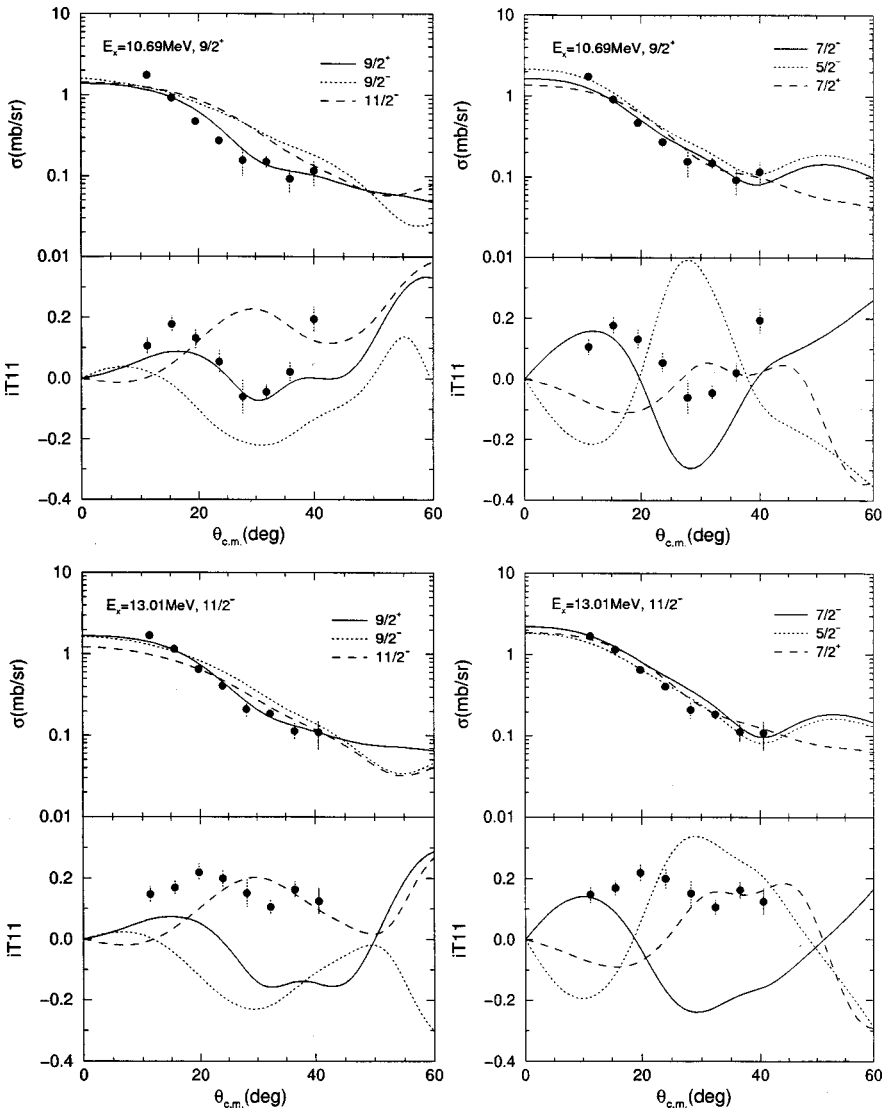

FIG. 5. ^{12}C(^{6}Li,^{3}He)^{15}N cross section and vector analyzing power data for transitions to the 10.69 MeV, $\frac{9}{2}^{+}$ and 13.01 MeV, $\frac{11}{2}^{-}$ states. The curves are the results of CCBA calculations with the assumed final state J^{π} value in ^{15}N shown.

core (α particle for ^{7}Li and ^{12}C for ^{15}N) with the appropriate binding energy. The geometry parameters of the bound state potentials are given in Table I. A slightly negative value for the binding energy was used in the calculations for the states which are at an excitation energy higher than the decay threshold (14.85 MeV) for $^{15}\mathrm{N}^{*}\rightarrow{}^{12}\mathrm{C}+t$.

For sometime now [24], it has been known that the reorientation of the ground state of ^{7}Li has a profound affect on ^{7}Li elastic scattering because of the large quadrupole moment of ^{7}Li. Whether ground state reorientation greatly modifies transfer angular distributions is still an open question. For the (^{7}Li,^{6}Li) reaction, inclusion of reorientation in CCBA calculations tends to dampen the structure in the angular distributions but does not change the overall shape of the distributions [25,26]. However, its inclusion is absolutely necessary for reproducing the nonzero rank 1 and 2 analyzing powers observed [26].

To determine whether projectile excitation and reorientation greatly modify calculated (^{7}Li,α) angular distributions, CCBA calculations have been carried out with the code FRESCO [27] for the ^{12}C(^{7}Li,α) reaction for several states with the following assumptions: (i) FRDWBA, meaning no projectile couplings, (ii) coupling between the $\frac{3}{2}^{-}$ ground and $\frac{1}{2}^{-}$ first excited states with ground state reorientation but no transfer from the $\frac{1}{2}^{-}$ state, and (iii) same as (ii) and including transfer from the $\frac{1}{2}^{-}$ state. The optical parameters listed in Table I were used in the calculations. These calculations for a $\frac{9}{2}^{+}$ state at 10.70 MeV and a $\frac{11}{2}^{-}$ state at 13.01 MeV are shown in Fig. 4, along with the calculated vector analyzing powers. As can be seen, there are only minor differences between the CCBA and FRDWBA angular distribution calculations. Since it has been shown in the past that measured vector analyzing powers for ^{7}Li induced single particle transfer reactions are sensitive to projectile excitation effects, calculated vector analyzing powers are also shown in Fig. 4. As can be seen, quite detailed measurements would be required to assess the role played by projectile excitation in the (^{7}Li,α) reaction. FRDWBA calculations were carried out for the rest of the ^{12}C(^{7}Li,α) study because the full set of projectile excitation data needed to carry out reliable CCBA calculations was not available.

Another possible test of the use of (^{7}Li,α) angular distributions to extract final state spin information is the ^{16}O(^{7}Li,α)^{19}F reaction to the ''well-known'' 2.78 MeV, $\frac{9}{2}^{+}$

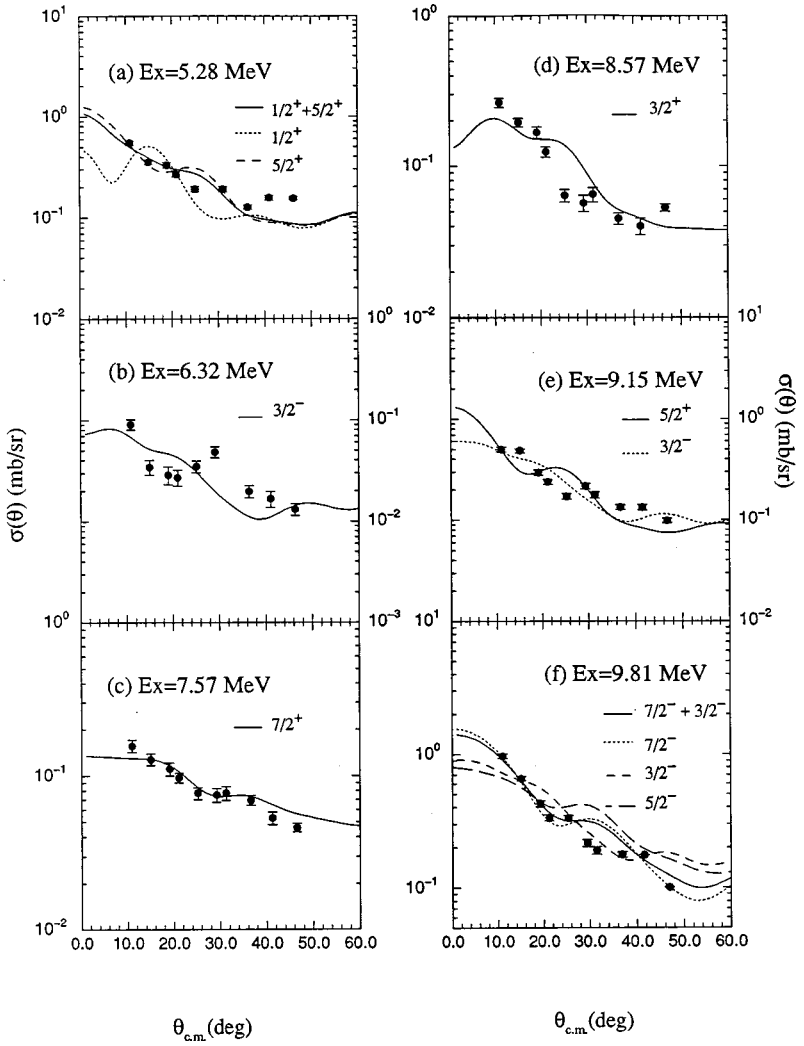

FIG. 6. Data and FRDWBA calculations for the ^{12}C(^{7}Li,α) reaction to states below 10.7 MeV for which J^π values are known.

and 4.65 MeV, $\frac{13}{2}^+$ states, for which, angular distributions have been reported for both peaks by Tserruya *et al.* [12]. Inspection of the two experimental angular distributions shows them to be completely different with the 2.78 MeV peak having a rather slowly changing cross section as a function of increasing angle as expected for a high spin state, whereas the 4.65 MeV angular distribution decreases rapidly as a function of increasing angle as expected for a lower spin state. The ^{16}O(^{7}Li,α) study of Mordechai and Fortune [13] suggests that both 4.65 ($\frac{13}{2}^+$) and 4.68 ($\frac{5}{2}^-$) states are excited in their 20 MeV work. Test calculations done in the present work show that the 2.78 MeV angular distribution is equally well described by a final state spin of $\frac{7}{2}^-$ or $\frac{9}{2}^+$ as expected from the ^{15}N analysis but that the 4.65 MeV peak is predominantly made up of the $\frac{5}{2}^-$ state rather than the $\frac{13}{2}^+$ state.

It would seem, then, that the angular distribution for the 4.65 MeV peak further strengthens the argument that the (^{7}Li,α) reaction populates negative parity states when compared with the (^{6}Li,^{3}He) and (α,p) reactions. The rather high level density in ^{19}F means that the only way to determine the actual states being populated by the different three-particle transfer reactions is to perform (^{7}Li,$\alpha\gamma$) and (^{6}Li,^{3}Heγ) studies as was done for ^{15}N [11]. Only then can there be a full understanding of the (^{7}Li,α) reaction.

B. ^{12}C($^6\vec{\text{Li}}$,^{3}He)^{15}N

Both FRDWBA (DWUCK5) and CCBA (FRESCO) calculations have also been carried out to study the possibility of using the vector analyzing power data from the ^{12}C($^6\vec{\text{Li}}$,^{3}He)^{15}N reaction to set limits on the J^π values for the states selectively populated. While it has been shown that the use of phenomenological Woods-Saxon potentials [28,29] can mock up the effects of channel coupling in elastic scattering and transfer reaction cross section angular distributions, the role played by projectile excitation in the calculation of analyzing powers is still understudy. While the FRESCO CCBA calculations are more time consuming than those using the FRDWBA, the CCBA calculations should be more reliable for extracting J^π values from the measured vector analyzing powers if the projectile excitation strength is known. Extensive cross section and analyzing power data now exists for the ^{6}Li+ ^{12}C system so that CCBA calculations can be performed for the ^{12}C($^6\vec{\text{Li}}$,^{3}He) reaction with the role played by projectile excitation determined from

TABLE II. The relative strengths of the doublets at 5.28 MeV and 9.81 MeV in ^{15}N.

Excitation of the doublet observed in this work	J^π state	Relative state strength
5.28 MeV	$\frac{5}{2}^+$; 5.270 MeV	73.5%
	$\frac{1}{2}^+$; 5.299 MeV	26.5%
9.81 MeV	$\frac{7}{2}^-$; 9.829 MeV	74.7%
	$\frac{3}{2}^-$; 9.925 MeV	25.3%

measured data [28,30] if sufficient computing resources are available. During the course of this work, several Pentium PC's running LINUX became available for running FRESCO CCBA calculations and so all calculations presented here have full channel coupling between the ground and excited states of ^{6}Li included. The CCBA calculations for the highest L values take about 1 h versus 5 min for the FRDWBA calculations. However, since up to seven computers have been available at various times for these calculations, it was possible to carry out the present study in a reasonable length of time. The optical model parameters used are given in Table I along with the bound state geometries needed. These parameters give a good description of the previously measured elastic cross section and analyzing powers for $E(^6\mathrm{Li}) = 50$ MeV. It was found that excitation of the target ^{12}C had no noticeable affect on the transfer calculations other than to increase the computing time and so target excitation was not included in the calculations shown in the following figures. The projectile excitation strengths were those taken from the inelastic scattering study of the $^6\mathrm{Li} + {}^{12}\mathrm{C}$ system of Kerr *et al.* [28]. The same bound state configurations and quantum numbers were used for $^{12}\mathrm{C}(^6\mathrm{Li},{}^3\mathrm{He})$ as those described earlier for the $(^7\mathrm{Li},\alpha)$ study. The conclusion reached as to the final J^π values extracted for the final states is the same for both sets of calculations, FRDWBA and CCBA, with only moderate differences between the calculated angular distributions and vector analyzing power shapes found for the two sets of calculations.

Again, test calculations were carried out for the known 10.69 MeV ($\frac{9}{2}^-$) and 13.01 MeV ($\frac{11}{2}^-$) states to determine whether the vector analyzing power data were sufficiently distinctive to determine the final state spins. As can be seen in Fig. 5, the 10.69 MeV data and calculations clearly pick out $\frac{9}{2}^+$ for this state with $\frac{7}{2}^-$ being the only other possibility.

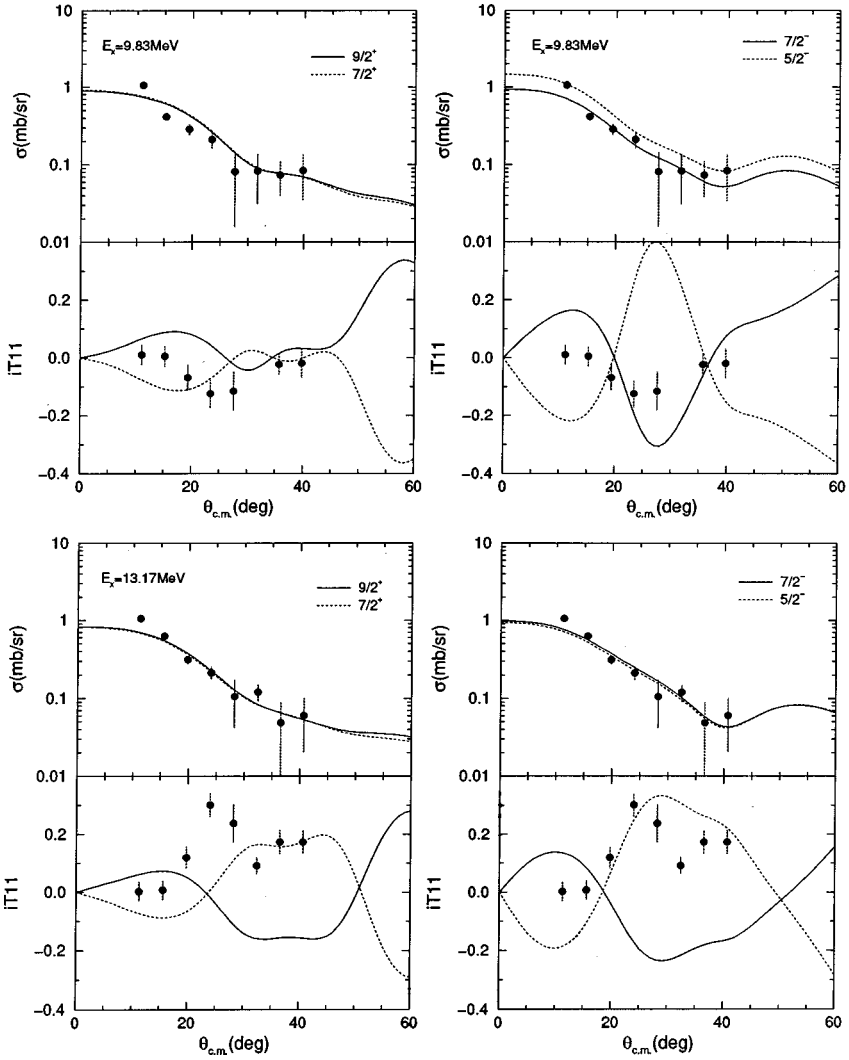

FIG. 7. Cross section and vector analyzing power data and CCBA calculations for peaks at 9.83 and 13.17 MeV populated in the $^{12}\mathrm{C}(^6\vec{\mathrm{Li}},{}^3\mathrm{He})^{15}\mathrm{N}$ reaction for $E(^6\mathrm{Li}) = 50$ MeV.

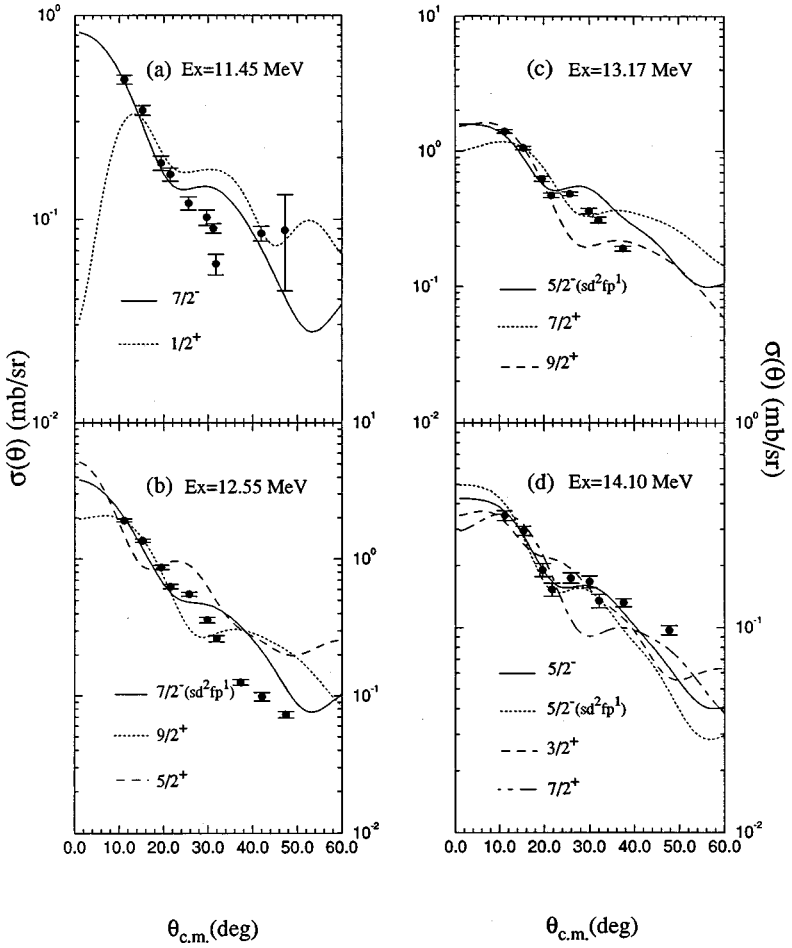

FIG. 8. Data and FRDWBA calculations for ^{12}C(^{7}Li,α) transitions to peaks at 11.45, 12.55, 13.17, and 14.10 MeV in ^{15}N.

The importance of the vector analyzing powers for extracting final state J^{π} values is also nicely shown in Fig. 5. For the 13.01 MeV state, the angular distribution data are consistent with spin-parities of $\frac{5}{2}^-$, $\frac{7}{2}^-$, $\frac{7}{2}^+$, $\frac{9}{2}^+$, $\frac{9}{2}^-$, and $\frac{11}{2}^-$. The combined angular distribution and vector analyzing power data are only consistent with an assignment of $\frac{11}{2}^-$ for this state.

V. RESULTS

The first step towards determining if the present data set could provide new information on the spectroscopy of states above the particle decay thresholds in ^{15}N($>$10.5 MeV) was to carry out FRDWBA calculations for states below 10.7 MeV. Good agreement between the data and (^{7}Li,α) calculations is obtained for the strong peaks at 5.28 ($\frac{5}{2}^+ + \frac{1}{2}^+$), 7.57 ($\frac{7}{2}^+$), 9.15 ($\frac{5}{2}^+$), and 9.83 ($\frac{7}{2}^-$) MeV. It is likely that both the $\frac{5}{2}^+$, 5.27 MeV and $\frac{1}{2}^+$, 5.30 MeV states are populated in the 5.28 MeV peak. As shown in Fig. 6, a combination of calculations for these states gives a better description of the data than does the calculation for each state separately. The angular distribution for the peak at 9.15 MeV is fit equally well with a $\frac{5}{2}^+$ (9.154 MeV) or $\frac{3}{2}^-$ (9.152 MeV) assignment in the current experiment. A previous particle gated γ-ray measurement using the ^{12}C(^{7}Li,$\alpha\gamma$) and ^{12}C(^{7}Li,^{3}Heγ) reactions [11,31] shows that it is the $\frac{5}{2}^+$ (9.154 MeV) state that is populated in this close-lying doublet. The better resolution spectrum of Zeller *et al.* [10] shows that the 9.83 ($\frac{7}{2}^-$), state is the dominant one populated in the triplet of states 9.76 ($\frac{5}{2}^-$), 9.83 ($\frac{7}{2}^-$), and 9.93 ($\frac{3}{2}^-$). In the present work and that of [10], the peak is broadened to high excitation, suggesting a small contribution from the $\frac{3}{2}^-$ state. An assumed doublet combination of 9.83 ($\frac{7}{2}^-$) and 9.93 MeV ($\frac{3}{2}^-$) reproduces the data quite well. The relative strengths of the states in the 5.28 and 9.83 MeV doublet combinations have been extracted by minimizing χ^2 and are listed in Table II.

As can be seen in Fig. 7, the ^{12}C($^{6}\vec{\text{Li}}$,^{3}He) angular distribution for the 9.83 MeV transition is consistent with both $\frac{7}{2}^-$ and $\frac{5}{2}^-$, but the predicted iT_{11} is widely different for $\theta_{\text{c.m.}} \approx 30°$ with $\frac{5}{2}^-$ transfer rising to $+0.4$ and a $\frac{7}{2}^-$ transfer having a value of -0.3. The negative experimental value of about -0.15 in this angular range then is consistent with a dominant population of the 9.83 MeV, $\frac{7}{2}^-$ state by the (^{6}Li,^{3}He) reaction also.

A recent work [32] reported a new $\frac{7}{2}^-$ level at 11.436 MeV. Until the work of Ref. [32], only a $\frac{1}{2}^+$ state at 11.438 MeV had been reported [33] close to this energy. While the two states are unresolved in the present work, the FRDWBA calculations and data given in Fig. 8 show that the $\frac{7}{2}^-$ state is the one strongly populated in the ^{12}C(^{7}Li,α) reaction.

The strong population of a peak at 12.55 MeV by the

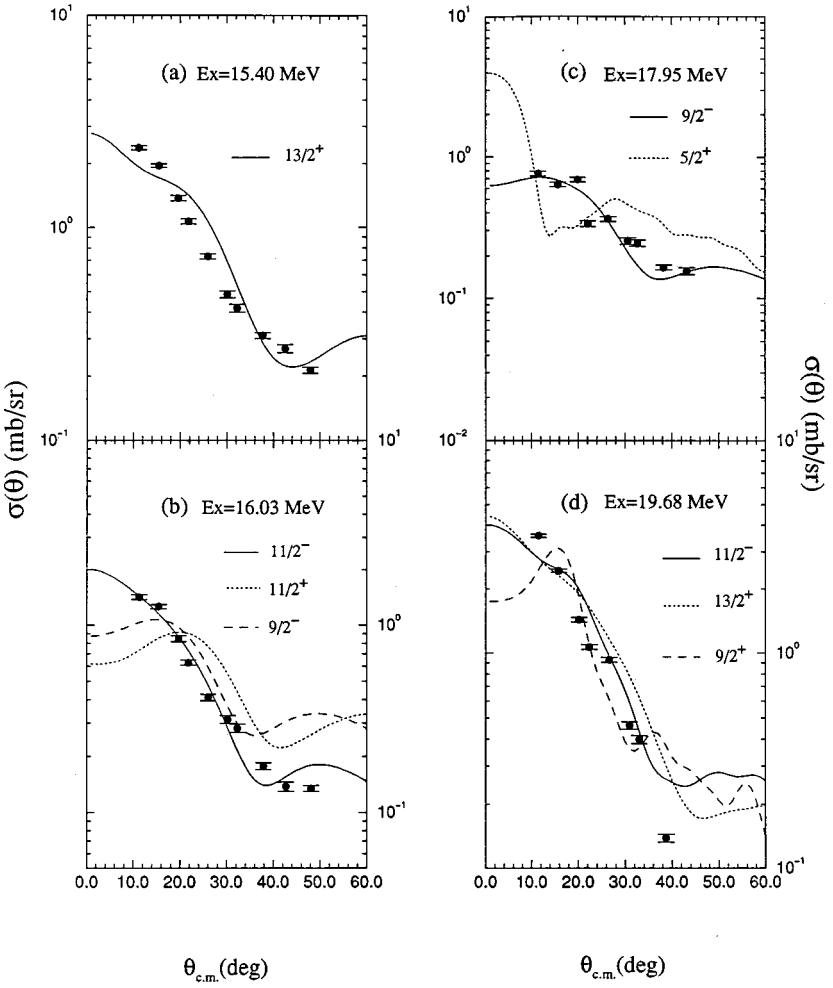

FIG. 9. Data and FRDWBA calculations for ^{12}C(^{7}Li,α) transitions to peaks at 15.40, 16.03, 17.95, and 19.68 MeV in ^{15}N.

^{12}C(^{7}Li,α) reaction provides the first evidence for major differences between this reaction and that of the (^{6}Li,^{3}He) and (α,p) reactions. In the latter two reactions, the population of this peak is weak relative to the ones at 13.01 and 10.69 MeV where as in ^{12}C(^{7}Li,α) it is stronger than either of these peaks. Two states around 12.5 MeV, one at an excitation energy of 12.522 MeV ($\frac{5}{2}^{+}$, $T=\frac{3}{2}$) and the other at 12.551 MeV ($\frac{9}{2}^{+}$), are reported in the most recent ^{15}N compilation [33]. A pion inelastic scattering study [34] assigns either $\frac{9}{2}^{+}$ or $\frac{7}{2}^{+}$ with $\frac{9}{2}^{+}$ favored for this state. An angular distribution and analyzing power measurement with the ($^{6}\vec{\text{Li}}$,^{3}He) reaction at a $^{6}\vec{\text{Li}}$ energy of 34 MeV [8] support an assignment of $\frac{9}{2}^{+}$ for the peak observed in that reaction. At the present bombarding energy of 50 MeV, the weak population of the peak at 12.55 MeV at larger angles, where the sensitivity to the transferred J^{π} is greatest does not allow the analyzing power data to be used to provide information about this peak. Since a strong population of a peak at 12.55 MeV appears only in the (^{7}Li,α) reaction, it is possible that the peak contains a state or states that are different from the $\frac{9}{2}^{+}$ state observed in other reactions. To test this idea, FRDWBA calculations were carried out for the ^{12}C(^{6}Li,^{3}He) reaction at 50 MeV, populating the 10.69 and 12.55 MeV states in ^{15}N. A relative spectroscopic factor of 1/0.31 was obtained for the 10.69/12.55 MeV states by comparing the calculations with the angular distribution data. When this ratio is applied to the ^{12}C(^{7}Li,α) FRDWBA calculations, the calculated 12.55 strength comes out to be only one-third of the observed strength. This result suggests that there are two close-by states at 12.55 MeV, one of $\frac{9}{2}^{+}$ and the other of undetermined spin and parity. Comparison with the nucleus ^{19}F would suggest $\frac{7}{2}^{-}$ for the major part of the 12.55 MeV strength with a configuration of $(sd)^{2}(fp)^{1}$. Calculations with this assumed configuration are shown in Fig. 8.

Perhaps one of the most difficult peaks to interpret in three-particle transfer reactions is that at 13.17 MeV. There is a doublet of narrow states known to exist [35], one at 13.149 MeV and the other at 13.174 MeV. High resolution ^{12}C(α,p) spectra show [36] the 13.174 MeV peak to be populated 10 times stronger than the one at 13.149 MeV. A recent better resolution ^{12}C(^{7}Li,α) α decay study of this region suggests the possibility of a triplet or quartet of states in this region [37]. One state is preferentially populated in the (^{7}Li,α) reaction and it is assumed in the present work that all three transfer reactions strongly populate the same state of 13.17 MeV in ^{15}N. There does not seem to be any practical way to experimentally test this assertion at present.

The peak at 13.17 MeV is weakly populated by the (^{6}Li,^{3}He) and (α,p) reactions but is strongly populated in (^{7}Li,α). Early works suggested a spin of $\frac{9}{2}$ [35] for this

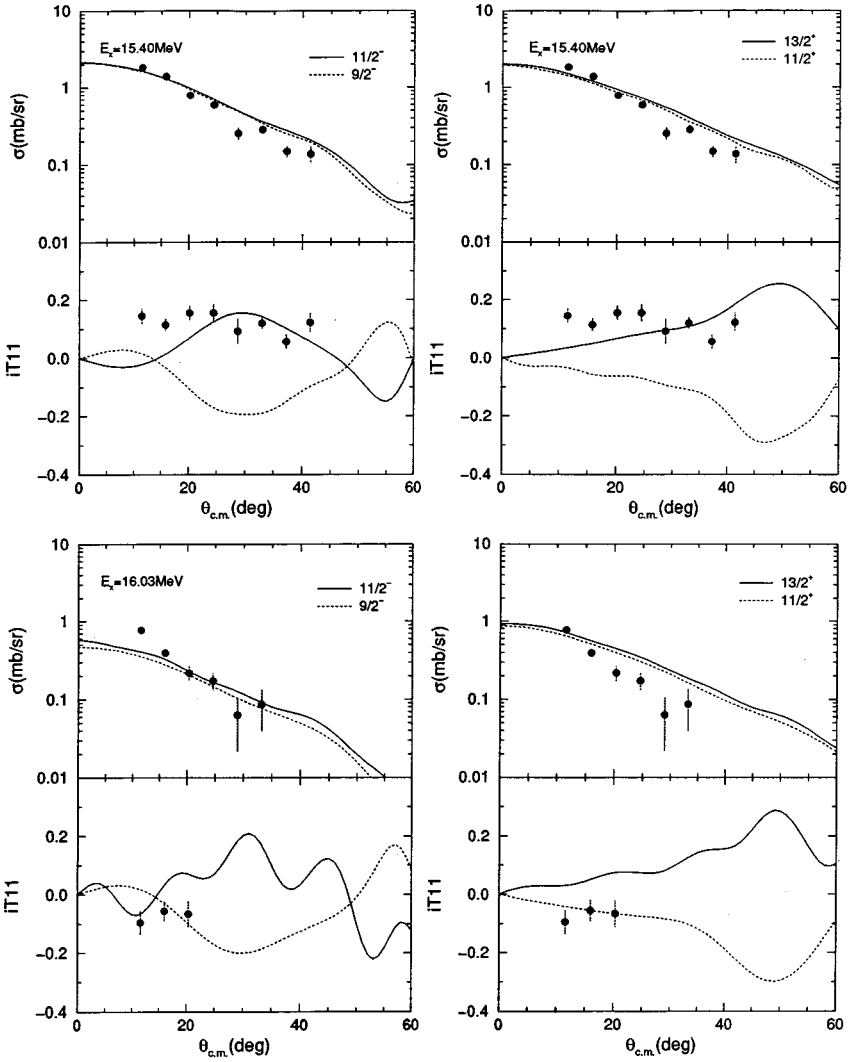

FIG. 10. Cross section and analyzing power data and CCBA calculations for ^{12}C($^{6}\vec{\text{Li}}$,^{3}He) transitions to states in ^{15}N at 15.40 and 16.03 MeV.

peak, but this spin is hard to reconcile with its relative population by the different three-particle transfer reactions. The strong population of this peak with the reasonably well angular momentum matched (^{7}Li,α) reaction argues for a relatively low spin for this peak. One of the primary motivations for the earlier ^{12}C($^{6}\vec{\text{Li}}$,^{3}He) study [8] was to learn if the vector analyzing power data could provide additional limits on possible spin values for a single state at this energy. The assumption of the population of a single state by the ^{12}C(^{6}Li,^{3}He) reaction was based on the similarity between the (α,p) and (^{6}Li,^{3}He) spectra. The data in Ref. [8] were consistent with either $\frac{7}{2}^+$ or $\frac{5}{2}^-$ for this state and the data clearly ruled out either $\frac{9}{2}^+$ or $\frac{9}{2}^-$ for it. Descriptions of the present 50 MeV angular distribution and analyzing power data, shown in Fig. 7, favor $\frac{5}{2}^-$ for this state assuming all three-particle transfer reactions strongly populate the same state. The ^{12}C(^{7}Li,α) data and calculations, shown in Fig. 8, also favor $\frac{5}{2}^-$ for this state. In both calculations a configuration of $(sd)^2(fp)^1$ is assumed for the bound state configuration because the 13.17 MeV state is not populated by either the ^{13}C(α,d) [38] or ^{13}C(^{6}Li,α) [39] reactions.

To gain confidence in the negative parity assignments for the 12.55 MeV and 13.17 MeV states, the known spectroscopic information for the mass 17 and 19 systems was examined. The compilation of nuclei with $A=16$–17 [40] shows possible $\frac{7}{2}^-$ and $\frac{5}{2}^-$ states in ^{17}O with the valence particle assigned to the $1f$ shell at excitation energies of 5.697 and 5.733 MeV, respectively, while they are at excitation energies of 5.672 and 5.682 MeV in ^{17}F. Since the ground states of these nuclei are $\frac{5}{2}^+$, the energy gap between the $d_{5/2}$ and $f_{7/2}$ shells appears to be about 5.7 MeV in the mass 17 system. Studies using the ^{18}O(^{3}He,d)^{19}F [41,42] and ^{16}O(^{7}Li,α)^{19}F [12] reactions suggested $(sd)^2f_{7/2}$ configurations at excitation energies of 4.00 ($\frac{7}{2}^-$) and 5.10 MeV ($\frac{5}{2}^-$) in ^{19}F. These results show the shell-energy difference in ^{19}F to be about 4.0 MeV. Correspondence between the ^{19}F and ^{15}N $3p$-$4h$ states has been carried out [18] by direct comparison of data for the ^{12}C(α,p)^{15}N and ^{16}O(α,p)^{19}F reactions. The $\frac{9}{2}^+$ state at 10.69 MeV excitation in ^{15}N was suggested to correspond to the $\frac{9}{2}^+$ state at 2.78 MeV in ^{19}F. Combining these results suggests that $\frac{7}{2}^-$ and $\frac{5}{2}^-$ states with $3p$-$4h$ structures will lie at excitation energies of 12.0 and 13.2 MeV, respectively, in ^{15}N, consistent with the present ^{12}C(^{7}Li,α) results.

The recent ^{15}N compilation [33] lists a pair of states at 14.10 MeV in ^{15}N: a ($\frac{9}{2}^+$ or $\frac{7}{2}^+$) state at 14.090 MeV and a $\frac{3}{2}^+$ state at 14.10 MeV. The present angular distribution data shown in Fig. 8 are not consistent with FRDWBA calculations that assume either $\frac{3}{2}^+$ or $\frac{7}{2}^+$ for this state, but are in agreement with an assumption of $\frac{5}{2}^-$ for it. Both $p^1(sd)^2$ and $(sd)^2(fp)^1$ configurations for the final state produce equivalent descriptions of the data. Studies of ^{19}F [12,41,42] have not reported any $\frac{5}{2}^-$ $(sd)^2(fp)^1$ states at an excitation energy ~ 6 MeV which would correspond to the ^{15}N state, suggesting a $p^1(sd)^2$ configuration for this state. A study comparing the selective population of ^{15}N states by the ^{12}C(^{7}Li,α)^{15}N and ^{13}C(^{6}Li,α)^{15}N reactions [39] reveals that the 14.10 MeV state carries considerable two-nucleon transfer strength, which then supports a negative parity $2p$-$3h$ configuration for this state.

Little spectroscopic information has been presented in previous studies of highly excited states in ^{15}N above the decay threshold to $^{12}C+t$ (14.85 MeV). Some of the states in this excitation-energy range such as those at 15.40 MeV, 16.03 MeV, 17.95 MeV, and 19.68 MeV are strongly populated by the ^{12}C(^{7}Li,α) reaction. FRDWBA calculations have been carried out for each peak with several different configurations. Even though these states are triton unbound, it is assumed that the spins of these states are so high that the large centrifugal potential produces a quasibound state. Consequently, slightly negative values were used for the binding energies in the calculations. The earliest three-particle transfer studies [2,7] with ^{12}C as a target showed strong population of a peak at 15.40 MeV in excitation and angular momentum mismatch conditions combined with cluster model calculations led to the conclusion that this peak was $\frac{13}{2}^+$ and had a stretched $(d_{5/2})^3$ configuration. Both the present (^{7}Li,α) and ($^6\vec{\text{Li}}$, ^{3}He) data are consistent with this assignment, as can be seen from the data and calculations in Figs. 9 and 10. Calculations have been carried out for the other peaks for which it was possible to extract angular distribution data. The 16.03 MeV data, shown in Figs. 9 and 10, are consistent with an $\frac{11}{2}^-$, $(sd)^2(fp)^1$ assignment. The 17.95 MeV state is assigned $\frac{9}{2}^-$ in the present work with that at 19.68 MeV consistent with $\frac{11}{2}^-$. While the latter two assignments are highly speculative, the negative parity assignment for them is probably not.

The FRDWBA calculations yield spectroscopic strength information in addition to transferred angular momentum information. The spectroscopic factor for the states in ^{15}N having a structure composed of $t+^{12}$C can be obtained from the DWUCK5, FRDWBA ^{12}C(^{7}Li,α) calculations, by relating the experimental cross section σ_{expt} to the calculated one, σ_{DW}, through the relation

$$\sigma_{\text{expt}} = C^2S_1 C S_2^2 \left(\frac{2J_f+1}{2J_i+1}\right)\sigma_{\text{DW}}, \tag{1}$$

where J_i and J_f are the target and residual nuclei spins and C^2S_1 is the $^7\text{Li}\rightarrow\alpha+t$ spectroscopic factor, and C^2S_2 is the one for $^{15}\text{N}\rightarrow{}^{12}\text{C}+t$. Here we have taken C^2S_1 to be 1. The spectroscopic factor C^2S_2 was obtained by normalizing $(2J_f+1)$ times the FRDWBA calculations to the experimental cross sections for each state. The absolute spectroscopic factors for this reaction are given in Table III. The ^{12}C(^{6}Li,^{3}He) absolute spectroscopic factors were obtained from the FRESCO calculations for this reaction by again normalizing the calculated cross sections to the data. In these calculations, the spectroscopic amplitude is one of the input parameters into the calculation, and its value was adjusted to match the experimental cross sections. The values of C^2S_2 obtained for this reaction are also given in Table III. Relative spectroscopic factors normalized to the one for the 10.69 MeV, $\frac{9}{2}^+$ state are also presented in Table III.

TABLE III. Triton cluster transfer spectroscopic factors for the ^{12}C(^{7}Li,α) and ^{12}C(^{6}Li,^{3}He) reactions.[a]

E_x [b]	J^π [b]	(^{7}Li,α) C^2S(abs)	(^{7}Li,α) C^2S(rel)	(^{6}Li,^{3}He) C^2S(abs)	(^{6}Li,^{3}He) C^2S(rel)
5.27	$\frac{5}{2}^+$	0.066	0.49		
5.30	$\frac{1}{2}^+$	0.038	0.28		
6.32	$\frac{3}{2}^-$	0.017	0.13		
7.57	$\frac{7}{2}^+$	0.052	0.39		
8.57	$\frac{3}{2}^+$	0.047	0.35		
9.15	$\frac{5}{2}^+$	0.062	0.46		
9.83	$\frac{7}{2}^-$	0.104	0.78	0.072	1.39
9.93	$\frac{3}{2}^-$	0.048	0.36		
10.69	$\frac{9}{2}^+$	0.134	1.00	0.052	1.00
11.45	$\frac{7}{2}^-$	0.043	0.32		
12.55	$\frac{7}{2}^-$ [c]	0.089	0.66		
	$\frac{9}{2}^+$	0.119	0.89		
13.01	$\frac{11}{2}^-$	0.232	1.73	0.071	1.36
13.17	$\frac{5}{2}^-$ [c]	0.141	1.05	0.176	3.40
14.10	$\frac{5}{2}^-$ [c]	0.032	0.24		
15.38	$\frac{13}{2}^+$	0.901	6.72	0.076	1.46
16.03	$\frac{11}{2}^-$ [c]	0.232	1.73	0.040	0.77
17.95	$\frac{9}{2}^-$ [c]	0.239	1.78		
19.68	$\frac{11}{2}^-$ [c]	0.518	3.87		

[a] C^2S for $^7\text{Li}\rightarrow\alpha+t$ and $^6\text{Li}\rightarrow{}^3\text{He}+t$ were assumed to be 1.
[b] Excitation energies and J^π values taken from Ref. [33].
[c] Proposed spin-parity values from the present work.

The (^{7}Li,α) values in Table III show that the states that have been suggested to have a large $t+^{12}$C cluster parentage, such as the 10.69 and 13.01 MeV states, have spectroscopic factors that are at least a factor of 8 larger than the 6.32 MeV, $\frac{3}{2}^-$ state, which has at best a very small triton cluster amplitude. Also, the (^{7}Li,α) calculated cross sections yield absolute spectroscopic factors that are reasonable in magnitude, indicating that the FRDWBA provides a reasonable description of this reaction. The absolute value of the spectroscopic factors derived from (^{6}Li,^{3}He) are about a factor of 3 smaller than those for (^{7}Li,α). Perhaps the most surprising result is the rather large spectroscopic factor obtained from both reactions for the 13.17 MeV state. Since all reaction analyses of this state suggest it has a maximum spin of $\frac{7}{2}$, it could mix with other lower spin states which would spread its cluster strength over several states, rather than hav-

ing it localized in a single state. Instead its strength is quite localized. The very early [2] identification of the 15.38 MeV peak as having a large *t* cluster configuration is quantitatively confirmed by the present work.

VI. DISCUSSION AND SUMMARY

The present work proposes that the $^{12}C(^7Li,\alpha)$ reaction preferentially populates negative parity states in ^{15}N. Several new J^π values are suggested with selective confirmation being provided by the present $^{12}C(\vec{^6Li},^3He)$ reaction study. A comparison with known levels in the mirror nucleus ^{15}O can also aid in understanding the levels in ^{15}N, when the ^{15}N level energies are shifted down by about 300 keV for ^{15}O [43]. There exist in ^{15}O several negative parity states [33] in the 11–12.5 MeV excitation region with no apparent mirror states known, suggesting the existence of unknown negative parity states in ^{15}N. However, the difficulty of trying to identify mirror states in ^{15}N-^{15}O is perhaps best illustrated by the 13.17 MeV state in ^{15}N. No mirror of this state has been found in ^{15}O. The similarity of the cross section magnitudes [7] for the summed 13.00 + 13.17 MeV peaks in ^{15}O and the 12.83 MeV peak in ^{15}O suggests that the mirror of the 13.17 MeV peak is degenerate with the 12.83 MeV peak in ^{15}O, so that it is extremely difficult to obtain information about the important 13.17 MeV ^{15}N state from a study of ^{15}O.

The present work also suggests that negative parity states with a dominant configuration of (sd^2f) have been observed above 13 MeV in excitation in ^{15}N. A shell model study [44] of negative parity levels in ^{15}N states that, on quite general grounds, the $f_{7/2}$ orbit should be important in forming states in the 13–15 MeV excitation region in ^{15}N, providing support to the present observation.

Knowledge of $3p$-$4h$ components in ^{15}N has been shown to be important for understanding even the lower excitation energy levels in ^{15}N [43,45]. However, it is difficult to reconcile the Alburger-Millener shell model calculation with our present experimental knowledge of ^{15}N since they predict a large $3p$-$4h$ component for the $\frac{1}{2}^+$ level at 9.05 MeV but its population in three-particle transfer reactions appears to be negligible [11].

The very selective population of states in ^{15}N by three-particle transfer reactions suggested that a comparatively simple $^{12}C+t$ and $^{11}B + \alpha$ cluster model [46] might be able to describe the spectrum of levels observed. An extension of this early work by Pilt [47] that includes knowledge gained from applying this model to levels in ^{19}F suggests that there should exist $\frac{7}{2}^-$ and $\frac{11}{2}^-$ (d^2f) cluster states at 16.2 and 18 MeV in ^{15}N, which is in reasonable agreement with the present work. The cluster model ideas are made more difficult in ^{15}N by the fact that the *t* and α cluster states are degenerate in energy in ^{15}N [11] whereas they are separated by several MeV in ^{19}F. As stated by Pilt [45], the high level density in ^{15}N makes it one of the most difficult nuclei to understand in terms of the cluster model.

In summary, the present work shows that FRDWBA calculations give a good description of $^{12}C(^7Li,\alpha)$ transfer angular distributions. Comparison between the present reaction study and the $^{16}O(^7Li,\alpha)$ reaction suggests that several of the strong levels observed in ^{15}N have negative parity. The very different population of levels by the $^{12}C(\vec{^6Li},^3He)$ reaction allowed confirmation of the $(^7Li,\alpha)$ proposed J^π values for only two levels. The present work clearly shows that further development of cluster models for light nuclei is needed.

This work was supported by the U.S. National Science Foundation and CONICIT, Grant No. PI-097 (Venezuela).

[1] H.G. Bingham, H.T. Fortune, J.D. Garrett, and R. Middleton, Phys. Rev. Lett. **26**, 448 (1971).
[2] D.K. Scott, P.N. Hudson, P.S. Fisher, C.U. Cardinal, N. Anyas-Weiss, A.D. Panagiotou, and P.J. Ellis, Phys. Rev. Lett. **28**, 1659 (1972).
[3] W.R. Falk, A. Djaloeis, and D. Ingham, Nucl. Phys. **A252**, 452 (1975).
[4] B. Buck, C.B. Dover, and J.P. Vary, Phys. Rev. C **11**, 1803 (1975).
[5] B. Buck and A.A. Pilt, Nucl. Phys. **A280**, 133 (1977).
[6] J.J. Hamill, R.J. Peterson, and D. Ingham, Nucl. Phys. **A252**, 452 (1975).
[7] H.G. Bingham, M.L. Halbert, D.C. Hensley, E. Newman, K.W. Kemper, and L.A. Charlton, Phys. Rev. C **11**, 1913 (1975).
[8] K.W. Kemper, P.L. Kerr, A.J. Mendez, E.G. Myers, K. Rusek, and G. Tungate, Phys. Lett. B **321**, 183 (1994).
[9] I. Tserruya, B. Rosner, and K. Bethge, Nucl. Phys. **A213**, 22 (1973).
[10] A.F. Zeller, K.W. Kemper, T.R. Ophel, and A. Johnston, Nucl. Phys. **A344**, 307 (1980).
[11] L.H. Harwood and K.W. Kemper, Phys. Rev. C **20**, 1383 (1979).
[12] I. Tserruya, B. Rosner, and K. Bethge, Nucl. Phys. **A235**, 75 (1974).
[13] S. Mordechai and H.T. Fortune, Phys. Rev. C **30**, 1924 (1984).
[14] L.M. Martz, S.J. Sanders, P.D. Parker, and C.B. Dover, Phys. Rev. C **20**, 1340 (1979).
[15] K. Van der Borg, R.J. de Meijer, and A. Van der Woude, Nucl. Phys. **A273**, 172 (1972).
[16] A.F. Zeller, K.W. Kemper, D.C. Weisser, T.R. Ophel, D.F. Hebbard, and A. Johnston, Nucl. Phys. **A323**, 477 (1979).
[17] P.L. Kerr, K.W. Kemper, P.V. Green, K. Mohajeri, E.G. Myers, D. Robson, and B.G. Schmidt, Phys. Rev. C **52**, 1924 (1995).
[18] K. Van der Borg, R.J. de Meijer, A. Van der Woude, and H.T. Fortune, Phys. Lett. **84B**, 51 (1979).
[19] A.A. Farra, Can. J. Phys. **74**, 150 (1996).
[20] P.D. Kunz, computer code DWUCK5 (unpublished).
[21] H. Oeschler, H. Fuchs, and H. Schröter, Nucl. Phys. **A202**, 513 (1973).

[22] V.I. Kukulin, V.G. Neudatchin, and Yu.F. Smirnov, Nucl. Phys. **A245**, 429 (1975).
[23] T. Kammuri and H. Yoshida, Nucl. Phys. **A129**, 625 (1969).
[24] V. Hnizdo, K.W. Kemper, and J. Szymakowski, Phys. Rev. Lett. **46**, 584 (1981).
[25] K.W. Kemper, G.A. Hall, S.P. Van Verst, and J. Cook, Phys. Rev. C **38**, 2664 (1988).
[26] I.M. Turkiewicz, Z. Moroz, K. Rusek, I.J. Thompson, R. Butsch, D. Kramer, W. Ott, E. Steffens, G. Tungate, K. Becker, K. Blatt, H.J. Jünsch, H. Leucher, and D. Fick, Nucl. Phys. **A486**, 152 (1988).
[27] I.J. Thompson, Comput. Phys. Rep. **7**, 167 (1981).
[28] P.L. Kerr, K.W. Kemper, P.V. Green, K. Mohajeri, E.G. Myers, and B.G. Schmidt, Phys. Rev. C **55**, 2441 (1997).
[29] D.P. Sanderson, S.P. Van Verst, J. Cook, K.W. Kemper, and J.S. Eck, Phys. Rev. C **32**, 887 (1985).
[30] P.L. Kerr, K.W. Kemper, P.V. Green, K. Mohajeri, E.G. Myers, B.G. Schmidt, and V. Hnizdo, Phys. Rev. C **54**, 1267 (1996).
[31] L.H. Harwood, K.W. Kemper, J.D. Fox, and A.H. Lumpkin, Phys. Rev. C **18**, 2145 (1978).
[32] T.R. Wang, R.B. Vogelaar, and R.W. Kavanaugh, Phys. Rev. C **43**, 883 (1991).
[33] F. Ajzenberg-Selove, Nucl. Phys. **A523**, 1 (1991).
[34] S.J. Seestrom-Morris, D. Dehnhard, C.L. Morris, L.C. Bland, R. Gilman, H.T. Fortune, D.J. Millener, D.P. Saunders, P.A. Seidi, R.R. Kiziah, and C.F. Moore, Phys. Rev. C **31**, 923 (1985).
[35] F. Ajzenberg-Selove, Nucl. Phys. **A449**, 1 (1986).
[36] J.D. Brown and K.W. Kemper (unpublished).
[37] C. Lee, D.D. Caussyn, N.R. Fletcher, D.L. Gay, M.B. Hopson, J.A. Liendo, S.H. Myers, M.A. Tiede, and J.W. Baker, Phys. Rev. C **58**, 1005 (1998).
[38] M. Yasue, J.J. Hamill, H.C. Bhang, M.A. Rumore, and R.J. Peterson, Phys. Rev. C **30**, 770 (1984).
[39] L.H. Harwood and K.W. Kemper, Phys. Rev. C **14**, 368 (1976).
[40] D.R. Tilley, H.R. Weller, and C.M. Cheves, Nucl. Phys. **A564**, 1 (1993).
[41] L.L. Green, C.O. Lennon, and I.M. Naqib, Nucl. Phys. **A142**, 137 (1970).
[42] C. Schmidt and H.H. Duhm, Nucl. Phys. **A155**, 644 (1970).
[43] S. Raman, E.T. Jurney, J.W. Starner, A. Kuronen, J. Keinonen, K. Nordlund, and D.J. Millener, Phys. Rev. C **50**, 682 (1994).
[44] S. Lie and T. Engeland, Nucl. Phys. **A267**, 123 (1976).
[45] D.E. Alburger and D.J. Millener, Phys. Rev. C **20**, 1891 (1979).
[46] B. Buck, C.B. Dover, and J.P. Vary, Phys. Rev. C **11**, 1803 (1975).
[47] A.A. Pilt, Nuovo Cimento A **74**, 185 (1983).